Remotely sensed spectral variability predicts reef fish diversity

A.C.B. Bakker [a,*], A.C.R. Gleason [b], A.C. Dempsey [c], S. Bachman [d], D. Burdick [e], A.M. Tarano [a], V. Chirayath [a], S.J. Purkis [a,c]

[a] *Rosenstiel School of Marine, Atmospheric, and Earth Science, University of Miami, Miami, FL, USA*
[b] *Department of Physics, University of Miami, Miami, FL, USA*
[c] *Khaled Bin Sultan Living Oceans Foundation, Annapolis, MD, USA*
[d] *Climate and Global Dynamics Laboratory, National Center for Atmospheric Research, Boulder, CO, USA*
[e] *Marine Laboratory, University of Guam, Mangilao, GU, USA*

ARTICLE INFO

ABSTRACT

In terrestrial landscapes, the spectral variability hypothesis (SVH) enables estimation of species diversity from satellite data, thereby allowing biodiversity assessments to be upscaled. Whether the SVH works in the marine realm is an open question. To answer it, we tested the ability of this hypothesis to retrieve coral reef fish biodiversity from two remote sensing platforms on a global transect of reef sites. From orbit, we trialed the multispectral and panchromatic bands of WorldView-2 (WV-2) which have a spatial resolution of 2.5 and 0.5 m, respectively. At 100 times finer resolution, we repeated the experiment using unpiloted aerial vehicle (UAV) data. Encouragingly, the SVH evidently works as well in water as has been reported on land. Spectral variability was positively correlated with fish diversity for all sensors, though the area in which the variability was computed (window size) was important. The strongest relationship between spectral variability and fish biodiversity (R = 0.48) was returned using UAV imagery corrected for surface artifacts via fluid lensing. Splitting fish into herbivores, corallivores, and piscivores revealed that different feeding strategies correlate to spectral variability at different scales. Based on our results, we contend that remote sensing data are underutilized when used to simply map benthic habitat. Spectral variation can clearly serve as a proxy for *in situ* reef biodiversity.

1. Introduction

Ecological theory contends that structural complexity promotes species diversity through niche generation (MacArthur and MacArthur 1961; Brown 1984; McElhinny et al. 2005; Stein et al. 2014). Tree cover and grassland patchiness, which affect bird species (Goetz et al. 2007; Lengyel et al. 2016), serve as excellent examples, as does seabed roughness mediating reef fish biodiversity (Gratwicke and Speight 2005; Purkis and Kohler 2008; Purkis et al. 2008; Graham and Nash 2013). Reef complexity also promotes resilience (Alvarez-Filip et al. 2009; Rogers et al. 2015; Yanovski et al. 2017), a sliver of hope against un-mitigated ecosystem collapse induced by bleaching, ocean acidification, and a myriad of other local and global anthropogenic insults (Syms and Jones 1998; Alvarez-Filip et al. 2009; Wilson et al. 2010; Riegl et al. 2012; Rogers et al. 2014).

Because coral reefs are vast and submerged, traditional *in situ* mea-surements of biodiversity are expensive and limited in spatial extent, requiring extensive SCUBA diver-based surveys. Remote sensing offers a complementary way to indirectly, but efficiently, survey biodiversity at scale. The spectral variation hypothesis (hereafter 'SVH'; Palmer et al., 1999) contends the spatial arrangement of organisms to be positively correlated with remotely sensed spectral variation (MacArthur and MacArthur, 1961; Palmer et al., 1999, 2002). This hypothesis has been used to audit species diversity in tropical forests (Carlson et al. 2007), wetlands (Heumann et al. 2015; Rocchini et al. 2017), grasslands (Rocchini et al., 2004, 2007, 2014; Hall et al., 2010, 2012), and, more recently, arctic tundra and boreal ecosystems (McPartland et al. 2019; Putkiranta et al. 2024). These authors have contributed to the validation of SVH over multiple spatial (10's to 10,000's of sq. m) and spectral (multispectral vs. hyperspectral) scales, focusing only on land plants. On reefs, spectral variation has been used to detect coral bleaching (Rowlands et al. 2008; Collin and Planes 2012; Li et al. 2020) and abundance of acroporid corals (Purkis et al. 2006), but not to measure biodiversity.

As the portfolio of studies that leverage the SVH grow, the debate continues as to the optimum metric of species diversity (Oldeland et al.

2010; i.e., abundance vs. count metrics), the appropriate scale to measure it at (Rocchini et al. 2007; Oldeland et al. 2010; Torresani et al. 2018; Gholizadeh et al. 2022; Pacheco-Labrador et al. 2022), and which ecosystems are well poised for the application of this hypothesis (Schmidtlein and Fassnacht 2017; Hauser et al. 2021; Fassnacht et al. 2022; Rossi et al. 2022; Torresani et al., 2024). Reef fish make for a compelling case study. They are pivotal to overall coral ecosystem health (Díaz-Pérez et al. 2016) and a critical source of protein for >one billion people (Kawarazuka and Béné 2011; Beveridge et al. 2013). In an effort to amplify the use of remote sensing for marine conservation, we aimed to test the SVH as a predictor of reef fish. We believed our work to be the first to use spectral variability as a reef ecosystem indicator. Though an imperfect comparison because they did not directly employ the SVH, the study by Cox et al. (2021) was noteworthy in its demonstration that fish diversity was correlated with the hue from photographs of corals. While the results from those authors were compelling, it remained to be tested whether remotely sensed imagery, as opposed to underwater images, could be used to assess fish diversity. Building forward from this, and the work in the terrestrial realm, we evaluated the SVH from two remote sensing platforms – at cm-scale from an unpiloted aerial vehicle (UAV) and at meter-scale from satellite. Our study was conducted on reefs distributed along a global transect spanning the Atlantic, Pacific, and Indian Oceans.

We pursued two aims. First, we tested whether the SVH can audit reef fish diversity. If it can, remote sensing has a role beyond simple habitat mapping in reef conservation. Satellites and drones could then also be used to audit ecosystem dynamics at scale. Our second aim was to identify the optimum spatial scales to lever the SVH. Due to its high spatial resolution and mode of acquisition, our UAV data allowed us to examine scale. We processed these data using 'fluid lensing' to remove spectral artifacts related to the sea surface, water column, and their effect on the underwater light field. This technology leveraged the distortion created by the ocean surface to magnify the seafloor, delivering imagery of unrivalled fidelity (Chirayath and Earle 2016; Chirayath and Li 2019). Multiple studies have emphasized reef fish to be sensitive to small-scale topography, which they used for hiding, foraging, and reproducing (Purkis et al. 2008; Wedding et al. 2019;

Fukunaga et al. 2020). Due to this behavior, we expected the strongest positive relationships between spectral variation and fish diversity to manifest at fine spatial scales, such as those afforded by fluid lensing.

2. Methods

2.1. A global transect

2.1.1. Global field data from the Living Oceans Foundation

Our study used two fish datasets collected by SCUBA divers. The first was gathered under the auspices of the Khaled bin Sultan Living Oceans Foundation Global Reef Expedition, hereafter 'KSLOF-GRE' (Purkis et al. 2019), which, between 2012 and 2015, counted fish at 720 stations across the Pacific, Indian, and Atlantic Oceans. Data were collected from hardbottom forereef and lagoonal habitats (Global Reef Expedition Final Report, 2021). The KSLOF-GRE field surveys were completed prior to the 2016–2017 global mass bleaching event, which negatively impacted reef fish diversity (Pratchett et al. 2018; Richardson et al. 2018). The 25 stations that had experienced recent local bleaching (degree heating week [DHW] >8 °C/week and eyewitness accounts) were excluded from our analysis, delivering a dataset comprised of 695 stations. Therefore, our work was agnostic to the effects of bleaching on the relationship between fish and spectral variability.

The KSLOF-GRE data were collected via the census method from English et al. (1997), where fish species were counted over 15-minute durations along 30 × 2-m transects. Each transect was conducted at five water depths (<8 m, 8–13 m, 14–18 m, 19–25 m, and >25 m), each with a minimum of four replicates. These replicates were averaged within each depth class, then averaged across the depths at which they were surveyed to yield a single fish count for each of the 695 stations. A full description of the KSLOF-GRE fish surveys has been detailed in both Purkis et al. (2019) and Bakker et al. (2022, 2024).

2.1.2. Tumon Bay field data from the Guam Long-term Coral Reef Monitoring Program

Our second fish dataset was collected in Tumon Bay as part of the Guam Long-term Coral Reef Monitoring Program (GLTMP) as part of the
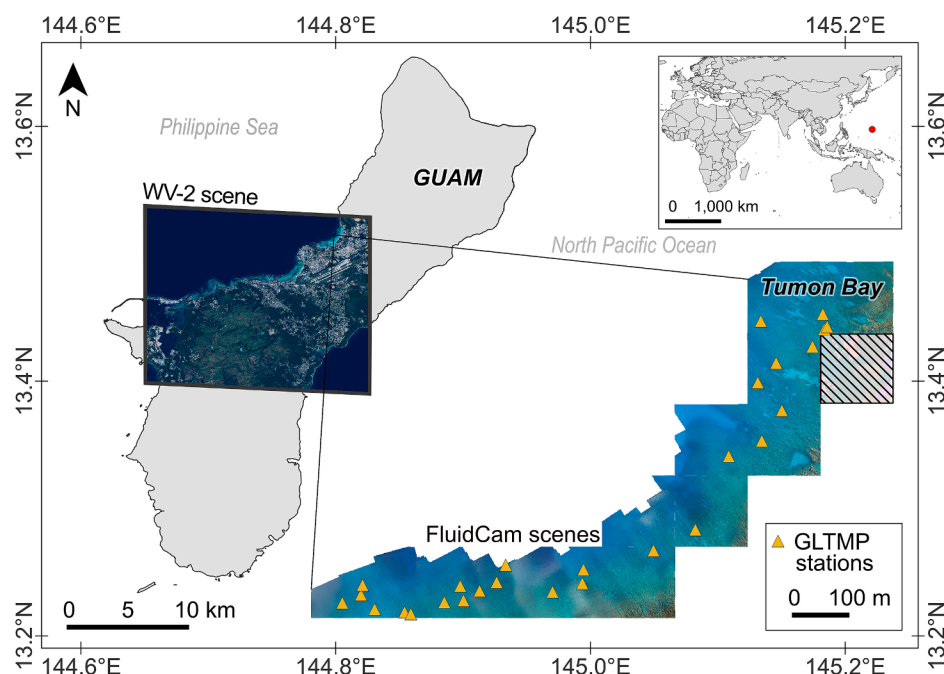

Fig. 1. Multi-scale remote sensing datasets assembled for Tumon Bay, Guam. One multispectral and one panchromatic scene from WorldView-2 ('WV-2') and 12 FluidCam scenes were used to image the 27 Guam Long-term Coral Reef Monitoring Program ('GLTMP') stations (orange triangles). The hatched FluidCam scene was used in Fig. 3 to show the Rao's Q calculation for each dataset.

NOAA Coral Reef Conservation Program jurisdictional cooperative agreement for Guam (Burdick et al. 2023). Here, fish were also counted on hardbottom habitat, on the outer reef slope terrace, between 7–15 m water depth. Although the GLTMP extends back to 2010, heat stress reached a record maximum in Tumon in 2017 (13 DHW), causing coral bleaching. No significant bleaching was recorded in subsequent years. In order to not introduce the bias of bleached reefs, we analyzed only the 27 GLTMP stations from 2019 to 2021.

The GLTMP surveyors utilized a stationary point-count method adapted from Ault et al. (2006) and the NOAA Pacific Islands Fisheries Science Center (Williams et al. 2011; Heenan et al. 2017) to identify fish species. Divers were positioned at 7.5 and 22.5 m along a 30-m transect, and each surveyor recorded all fish observed within a 7.5-m radius cylinder extending from their position along the transect. Fish were recorded during a 5-min listing phase, then the divers counted and sized each taxon during rapid visual sweeps of the plot (Burdick et al. 2023 and University of Guam Marine Laboratory, 2019 for details).

To ensure that the fish counts were consistent between the KSLOF-GRE and GLTMP surveys, all sharks, rays, eels, and cryptic fish, or fish <5 cm long, were excluded from both datasets. We further removed all KSLOF-GRE transects acquired deeper than 15 m (n = 170) because of the excessive attenuation of the visible-spectrum in our remote sensing dataset beyond this depth (Purkis and Chirayath 2022). Removing these deep stations resulted in a total 525 KSLOF-GRE stations, while we kept all 27 from the GLTMP.

2.2. Quantifying fish diversity

The fish data provided by the KSLOF-GRE and GLTMP allowed us to calculate diversity metrics related to species richness and evenness. Richness of fish species was represented by the number of observed species counted at each diver station, regardless of abundance. This metric thus placed the same weight on rare species as on dominant ones and was calculated for all fish from the KSLOF-GRE and GLTMP surveys, hereafter referred to as 'fish richness.'

Next, the diversity of fish species was assessed using Shannon's Index (Shannon 1948), which weights species based on their frequency. Shannon's diversity (H') was calculated via,

$$H' = -\Sigma p ln(p) \tag{1}$$

where p was the proportion of a given fish species per total species for each diver station. We referred to this metric as 'Shannon's diversity of fish.' We pursued two fish diversity metrics to ascertain which one afforded the strongest correlation with spectral variation, as has been done in previous terrestrial SVH studies (i.e., Oldeland et al. 2010).

2.3. Four remote sensing datasets

The first two satellite imagery datasets that we assembled, multispectral and panchromatic WorldView-2 (WV-2), spanned our two largest spatial scales. WV-2 Standard Level 2A surface reflectance products were already georeferenced, orthorectified, and radiometrically and atmospherically corrected (DigitalGlobe 2021; Fig. 1). These imagery boasted eight spectral bands (coastal blue, blue, green, yellow, red, red edge, and near-infrared 1 and 2) with a spatial resolution of 2.5 m, plus a single panchromatic band with 0.5 m resolution. Of the eight multispectral bands, we only utilized Bands 1 through 5, which penetrate water. All WV-2 scenes were acquired from within eight weeks of the KSLOF-GRE and GLTMP field survey dates, while maintaining <10 % cloud cover, and look angles <5° off-nadir, so as to minimize sun glint. These selection criteria delivered 2.5 m multispectral WV-2 imagery for 223 KSLOF-GRE stations and for 27 GLTMP stations, plus 0.5 m WV-2 panchromatic imagery for 112 KSLOF-GRE and 27 GLTMP stations. The total area of imagery assembled for this project was 99,850 sq. km.

While the optical effect of submergence in multispectral satellite imagery can be addressed using physics-based, semi-analytical, or empirical approaches (Lyzenga 1978; Lee et al. 1999; Green et al. 2000; Stumpf et al. 2003; Hedley et al. 2004; Kerr and Purkis 2018; Kutser et al. 2020), we deliberately chose not to apply such water column corrections to our WV-2 imagery. This decision was driven by two main factors. First, the spatial variability of the ocean's inherent optical properties made it difficult to scale these correction methods from individual satellite scenes to global remote sensing efforts. Additional challenges arise from differences in solar geometry, atmospheric clarity, and sea state between adjacent images, which complicate large-scale water column corrections. Given our goal of significantly scaling-up reef fish biodiversity assessments with remote sensing, we opted not to burden our deployment of the SVH with this additional image-processing step. The second reason was central to the SVH itself. The hypothesis holds predictive power because it serves as a proxy for niche generation within ecosystems. In this context, variations in water depth may be considered part of the signal rather than noise to be corrected. After all, there is compelling evidence that depth variations contribute to the creation of niches for reef fish (Purkis et al. 2008; Jankowski et al. 2015).

Our third and fourth datasets came from UAV-mounted FluidCam which utilized fluid lensing of high framerate multispectral imagery to resolve the seabed at cm-scale (Chirayath and Instrella 2019; Purkis and Chirayath 2022; Fig. 1). As visible light interacted with the sea surface, time-dependent nonlinear optical aberrations appear, forming intense bands of light on the seafloor, termed 'caustics', that produce a refractive lensing which magnifies and demagnifies underwater objects (Chirayath and Earle 2016). These caustic refractive distortions were exploited by the fluid lensing process to determine the 3D structure of the seafloor, to enhance the signal-to-noise ratio of the imagery, and to increase its effective spatial resolution by magnifying the wave events on the sea surface. Fluid lensing effectively removed refractive distortion from the ocean waves and produced the third benthic imagery product that we used for this study. To compliment this high-resolution product, we also kept the raw UAV imagery as our fourth, and final, remote sensing dataset. These UAV images have the finest spatial resolution of our assembled data (0.014 m).

Our four remote sensing datasets allowed us to test the SVH with imagery spanning >two orders of magnitude in spatial resolution (0.014 m to 2.5 m) and spanning between one and five spectral bands. The raw UAV imagery further allowed us to assess how fluid lensing corrections helped or hindered the SVH.

2.4. Spectral variability from Rao's Q

To calculate the spectral variability of our satellite and UAV imagery, we used the Rao's Q metric proposed by Rocchini et al. (2017), as recently employed by Khare et al. (2019) and Torresani et al. (2019) for terrestrial forests. Rao's Q accounted for both the proportion and the spectral distance of brightness values in an image by,

$$Q = \frac{1}{N^2} \sum_i \sum_j \sum_\alpha \left[\left(\Phi_{i,\alpha} - \Phi_{j,\alpha} \right)^2 \right]^{1/2} \tag{2}$$

where N was the number of pixels in an image, $i, j \in \{1, 2, ..., N\}$ represented the indices of individual pixels in that image, such that the first two summations were taken over all possible pairs of pixels, and Φ was the reflectance value taken from each band, α, of the WV-2 multispectral, WV-2 panchromatic, and UAV imagery. The Rao's Q formula which we used was thus a multidimensional Euclidean distance metric, and equivalent to the form presented in Rocchini et al. (2017) in the limit where the dissimilarity coefficient d was equal to the summand in Eq. (2) and the expression was renormalized so that probability p of sampling any pixel was simply one. Conveniently, the Rao's Q algorithm was highly parallelizable and we accordingly developed a program in
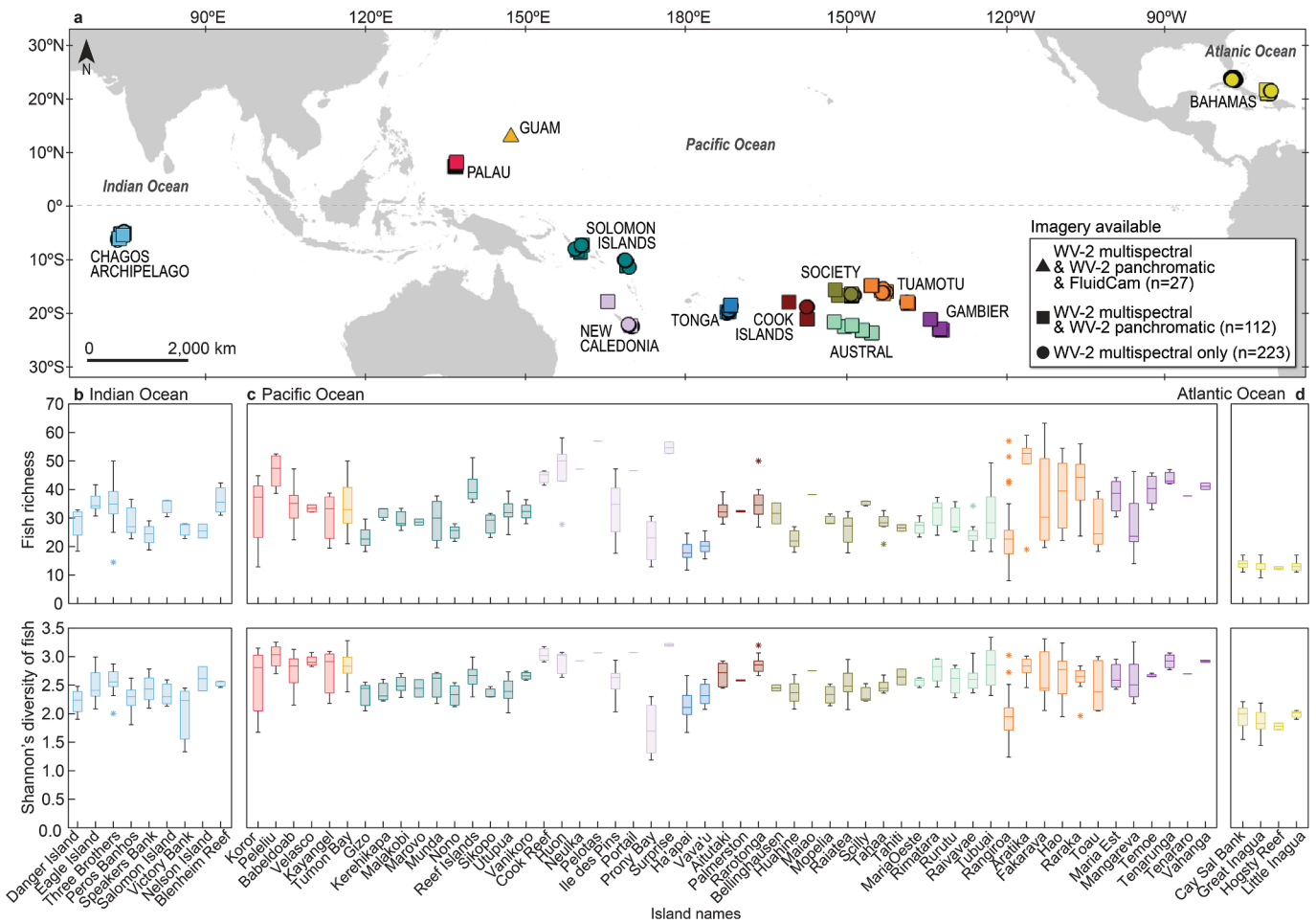
Fig. 2. Map of the **(a)** 250 dive stations from the KSLOF-GRE (n = 223) and GLTMP (n = 27) stations where SCUBA divers counted fish, and we assembled WorldView-2 (WV-2) multispectral (circles, triangles, and squares), WV-2 panchromatic (triangles and squares), and FluidCam imagery (triangles only). The KSLOF-GRE field surveys were completed between 2011–2015 and the GLTMP surveys between 2019–2021. The species richness and Shannon's diversity of reef fish were represented from east to west by box-and-whisker plots for the **(b)** Indian Ocean, **(c)** Pacific Ocean, and **(d)** Atlantic Ocean. An individual box represented fish diversity at the stations from a single island and boxes were colored by the archipelago to which the island belonged. Note lower fish diversity in the Atlantic as compared to the Pacific or Indian Oceans.

Chapel, 'RapidQ,' to accelerate the calculation of spectral variability over large areas (next section), spectral bands, and multispectral space (Bachman et al. 2023). Units of Rao's Q were relative to the input imagery; however, we did not compare imagery to imagery (only imagery to fish diversity), so the units were irrelevant to this study.

2.5. Spectral variability within windows

We computed Rao's Q on defined subsets, hereafter 'windows,' of remote sensing imagery centered at each station where fish had been counted. Iterative variation of window size allowed the SVH to be tested at different spatial scales. We computed Rao's Q within windows encompassing areas of 50, 25, 10, 5, 1, and 0.5 hectares (ha) for our WV-2 multispectral imagery, windows with 25, 10, 5, 1, 0.5, and 0.1 ha for our WV-2 panchromatic imagery, and windows with 0.005, 0.001, 0.0005, 0.0001, 0.00005, and 0.00001 ha for our finest resolution UAV-acquired imagery. Each of the six windows across datasets encompassed a similar ratio of pixels to window size. For example, the smallest WV-2 and UAV windows, 0.5 and 0.00001 ha, were comprised of 780 and 510 pixels, respectively.

Although there were no previous studies correlating fish diversity to spectral variability for us to base our window sizes on, there was evidence of fish responding to habitat diversity at large windows (50–300 ha; Dalleau et al. 2010; Olds et al. 2012; van Lier et al. 2018; Hale et al.

2019; Sievers et al. 2020; Bakker et al. 2024). The time to run the Rao's Q calculator, however, scaled with the square of the window size, and due to usage policies on our supercomputing cluster, we were unable to run any computations that took longer than twelve hours of walltime. Our largest window size (50 ha) reflected this limitation. The smallest window sizes for each imagery were large enough to incorporate a 10-pixel radius around the dive stations.

As previously described, the fish counts were conducted along transects. Hence, each count did not have a unique geographic position. To account for the area encompassed by each diver measurement, we calculated spectral variability from five randomized points within a radius of 15 m, centered on the mid-point of the 30 m transects along which the SCUBA divers had counted the fish. This approach allowed error to be estimated for spectral variability.

2.6. Correlating spectral variation with fish diversity

Using a Moran's I spatial autocorrelation test, we confirmed that variations in fish richness and Shannon's diversity were not a product of the spatial distribution of the SCUBA stations. We then performed linear correlation tests to evaluate the relationships between fish richness and Shannon's diversity, as measured at the 223 KSLOF-GRE and 27 GLTMP stations, with spectral variability computed from WV-2 (multispectral + panchromatic) and UAV imagery (raw + fluid lensed). Because of the
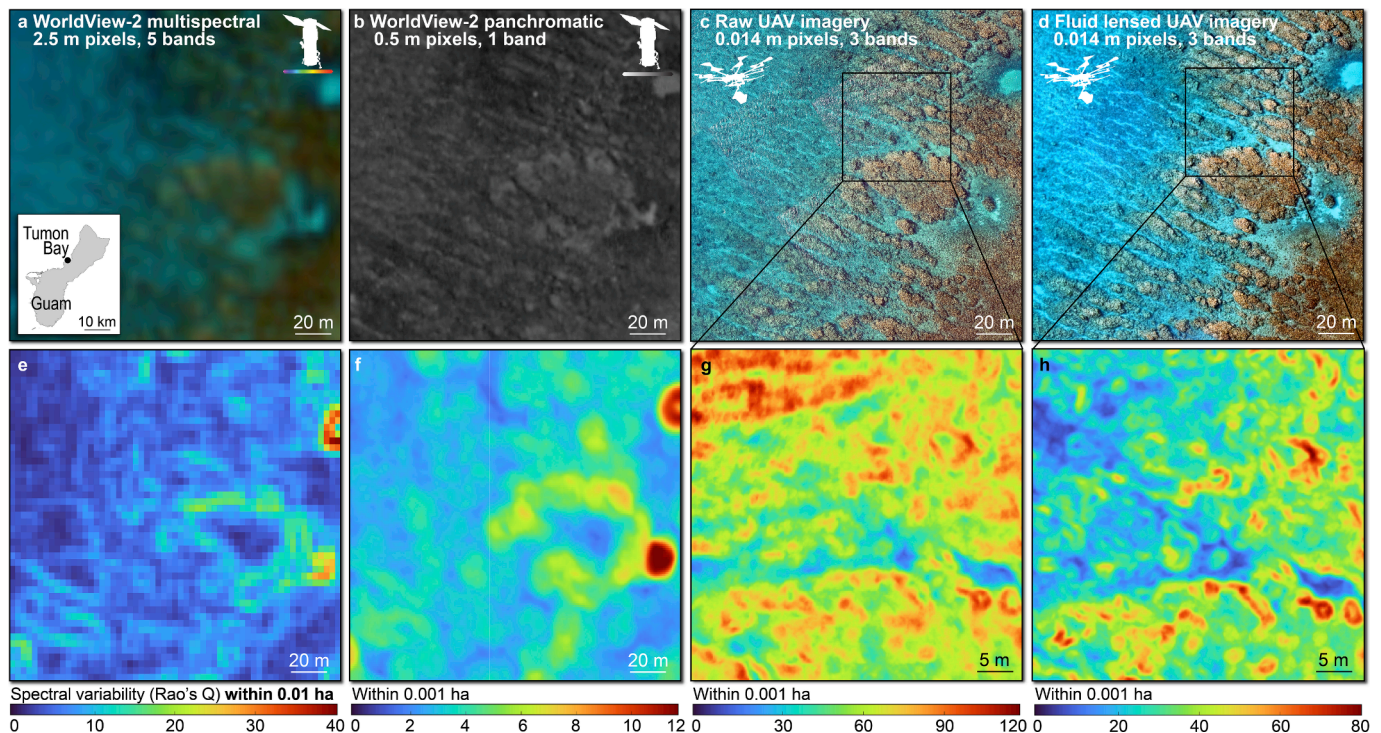
Fig. 3. An example from Tumon Bay, Guam, showing the spectral variability (Rao's Q) calculated from four types of remote sensing imagery: WorldView-2 (**[a]** five multispectral bands + **[b]** one panchromatic band) and FluidCam (three **[c]** raw + **[d]** fluid lensed bands). Rao's Q was calculated for the smallest 0.01 ha window on the **(e)** WV-2 multispectral image, and 0.001 ha for the **(f)** WV-2 panchromatic image and **(g-h)** two fluid lensing images. Both FluidCam heat maps **(g-h)** were magnified to resolve the fine-scale changes in spectral variability. The 0.01 and 0.001 ha windows corresponded to an area of 100 and 10 sq. m, respectively.

differences in how the fish were counted by KSLOF and GLTMP, we evaluated the SVH separately for the two datasets.

Correlation tests were repeated for Rao's Q calculated within each of our six window sizes for each of the four remote sensing datasets. While more complex regressions were available to us, we deliberately chose a linear relationship as this was the first experiment to test the SVH for reef fish. In future work, more complex (non-linear, machine learning, etc.) approaches might be taken. A significance level (alpha) of 0.01 was chosen to evaluate these correlation tests when our sample size was >100 (KSLOF-GRE). We adjusted the significance level to 0.05 for tests with sample sizes <100 (GLTMP). Correlation coefficients were assessed to determine which window size, remote sensor, and fish diversity metric correlated most strongly with spectral variation.

2.7. Fish family response to spectral variability

To tease apart how the SVH performed for fishes with different life strategies, we grouped our fish counts into herbivores (parrotfish, damsels, and tangs), benthic carnivores and corallivores (butterflyfish, squirrelfish, wrasse), and piscivores (grunts and grouper), then individually correlated those groupings against spectral variability. The range of window sizes afforded by our satellite data encompassed a large enough area to accommodate the various home ranges of these fish families (Almany et al., 2007; Green et al., 2015). We did not relate fish counts to UAV-derived spectral variability because the windows were too small to encompass a meaningful home range for the fish.

3. Results

3.1. A global reef fish and remote sensing dataset

Our SCUBA diver datasets were collected along a global transect through the Indian, Pacific, and Atlantic Oceans, with a broad range in fish species richness and Shannon's diversity measured at each of the

223 KSLOF-GRE and 27 GLTMP stations (Fig. 2). Of the 250 stations which we considered, four remote sensing technologies (WV-2 satellite multispectral and panchromatic, and fluid lensed and raw UAV imagery) could be assembled over 27 stations. Multispectral and panchromatic satellite data covered 112 stations, and 223 stations were solely imaged by multispectral satellite data (Fig. 2a). The richness and Shannon's diversity of fish were highest in the Indian and Pacific Oceans (Fig. 2b and c) relative to that measured in the Atlantic Ocean (Fig. 2d). Our 250 dive stations were paired with each of the corresponding remote sensing datasets (Fig. 1), and the spectral variability from the imagery surrounding that station was calculated.

3.2. Rao's Q as a measure of spectral variability

We provided an example to display the differences in calculating Rao's Q from our four datasets (Fig. 3). Here, we showed the spectral variability in the forereef of Tumon Bay in Guam (Fig. 3a–d) within a 0.01 ha window for WV-2 multispectral imagery and a 0.001 ha window for the other three datasets. Rao's Q measured the 'spectral dissimilarity' in an image and was therefore scaled to the spectral values and bands in that image. In this example, the highest Rao's Q values were obtained from the UAV data, which were stored as digital numbers, compared to the lower Rao's Q from reflectance values in WV-2 data. In the raw UAV imagery, waves and sun glint corresponded to areas with high Rao's Q (Fig. 3g; Rao's Q > 60). Otherwise, high Rao's Q corresponded to the edges between spectrally dissimilar benthic habitats, respectively for each image.

3.3. Spectral variability correlated with fish diversity

For each of our four image datasets, we calculated spectral variability within six different window sizes and correlated those results with fish richness and Shannon's diversity (Table 1). First, we examined the global KSLOF-GRE stations (Table 1a). The strongest positive

Table 1

Correlations between fish diversity and spectral variability from four imagery across our **(a)** KSLOF-GRE and **(b)** GLTMP stations. Results are shown for computing spectral variability within window sizes ranging from 0.5-50 ha for WorldView-2 (WV-2) multispectral imagery, 0.1–25 ha for WV-2 panchromatic imagery, and 0.00001–0.005 ha for UAV imagery, with a total of 223, 112, and 27 stations, respectively. Correlation coefficients (R) were provided for the relationship between spectral variability with both reef fish richness and Shannon's diversity. Significance levels indicated difference from zero and bolded for *** 0.0001/0.0005, ** 0.001/0.005, and * 0.01/0.05, while ns = not statistically significant. Window sizes where correlations were both bolded and underlined were carried forward for further analysis.

a Khaled bin Sultan Living Oceans Foundation Global Reef Expedition

WorldView-2 multispectral (n = 233)			WorldView-2 panchromatic (n = 112)		
Window (ha)	Richness (R)	Shannon's (R)	Window (ha)	Richness (R)	Shannon's (R)
0.5	**0.20**	**0.18***	0.1	0.05 (ns)	0.13 (ns)
1	**0.24***	**0.21***	0.5	0.10 (ns)	**0.25***
5	**0.36***	**0.30***	1	0.15 (ns)	**0.31***
10	**<u>0.38***</u>	**0.33***	5	**0.30***	**0.43***
25	**0.37***	**<u>0.34***</u>	10	**<u>0.31**</u>	**<u>0.44***</u>
50	**0.36***	**0.33***	25	**0.26***	**0.41***

b Guam Long-term Coral Reef Monitoring Program

WorldView-2 multispectral (n = 27)			WorldView-2 panchromatic (n = 27)		
Window (ha)	Richness (R)	Shannon's (R)	Window (ha)	Richness (R)	Shannon's (R)
0.5	−0.04 (ns)	−0.33 (ns)	0.1	0.06 (ns)	−0.19 (ns)
1	−0.03 (ns)	−0.31 (ns)	0.5	0.21 (ns)	−0.19 (ns)
5	0.07 (ns)	−0.16 (ns)	1	0.13 (ns)	−0.20 (ns)
10	0.30 (ns)	0.03 (ns)	5	0.24 (ns)	0.05 (ns)
25	0.33 (ns)	0.14 (ns)	10	0.32 (ns)	0.14 (ns)
50	0.30 (ns)	0.14 (ns)	25	0.30 (ns)	0.19 (ns)

Raw UAV imagery (n = 27)			Fluid lensed UAV imagery (n = 27)		
Window (ha)	Richness (R)	Shannon's (R)	Window (ha)	Richness (R)	Shannon's (R)
0.00001	0.08 (ns)	0.36 (ns)	0.00001	**0.40***	0.01 (ns)
0.00005	0.09 (ns)	0.33 (ns)	0.00005	**0.42***	−0.11 (ns)
0.0001	0.11 (ns)	0.33 (ns)	0.0001	**0.43***	−0.16 (ns)
0.0005	0.11 (ns)	0.33 (ns)	0.0005	**0.45***	−0.25 (ns)
0.001	0.12 (ns)	0.30 (ns)	0.001	**0.45***	−0.24 (ns)
0.005	0.11 (ns)	0.27 (ns)	0.005	**<u>0.48*</u>	−0.18 (ns)

relationship between fish richness and WV-2 multispectral variability was found using the 10-ha window (R = 0.38), which was only slightly more positive than the strongest correlation to Shannon's diversity of fish at a 25-ha window (R = 0.34). When computing spectral variability from WV-2 panchromatic imagery, the strongest relationship to fish richness was found using the 10-ha window (R = 0.31). For Shannon's diversity, meanwhile, the strongest result was returned at the same window size (R = 0.44).

Tested next were the relationships between spectral variability and fish diversity from the 27 GLTMP stations in Tumon Bay. Regardless of window size, no significant relationships to either fish richness or Shannon's diversity were found when spectral variability was computed using WV-2 multispectral, WV-2 panchromatic, or raw UAV imagery. Neither were any significant relationships found when correlating Shannon's diversity of fish with spectral variability of fluid lensed imagery. However, the strongest positive relationship across all of our tests (KSLOF-GRE and GLTMP) was found when correlating fish richness with fluid lensed imagery within the 0.005 ha window (R = 0.48, Table 1b). For the remainder of our analysis, we used the combination of fish diversity metrics and sensor type that delivered the strongest correlations (bolded and underlined in Table 1).

Fig. 3 split the KSLOF-GRE fish counts into three depth bins: Depth 1 (<13 m), D2 (13–15.5 m), and D3 (>15.5 m). When spectral variability was computed from multispectral WV-2, the strongest correlations occur in the shallowest bin (R = 0.47 with fish richness, and 0.39 for Shannon's diversity of fish; Fig. 4a). The deepest depth bin returned the lowest correlation in both cases. No significant correlations were returned from D1 when the same experiment was conducted for the panchromatic WV-2 imagery (Fig. 4b), and the highest correlations were found in D3 with fish richness (R = 0.51) and Shannon's diversity of fish (R = 0.56).

Next, we showed the correlation between fish richness and spectral diversity calculated from fluid lensed data (Fig. 5). Although all window sizes for this test produced significant correlations (Table 1b), the largest 0.05 ha window returned the highest correlation (R = 0.48). There were no significant correlations when using Shannon's diversity of fish, or when calculating spectral variability from the raw UAV data. Also, the 27 GLTMP stations did not provide satisfactory statistical power to test the effect of depth on correlation strength.

3.4. Correlation strength is dependent on fish feeding strategy

Our final analysis examined whether the SVH extracted from WV-2 multispectral imagery was effected by splitting our fish counts into three functional groups. The correlation strength for all fish groups within windows sized 0.01 to 50 ha was shown as a red dashed line in Fig. 6a, where the herbivores were shown in green, benthic carnivores and corallivores in blue, and piscivores in orange. The correlation strength between both herbivores and corallivores and spectral variability peaked at windows ranging from 0.5 to 50 ha, while the piscivores showed peak correlations at a much narrow range, between 0.5 to 1 ha (Fig. 6b). Parrotfish, butterflyfish, and grunts had their strongest positive correlations to spectral variability at 0.5 ha, while those strongest correlations were at 50 ha for wrasse, tangs, and damselfish. Only grouper and tangs exhibited negative correlations to spectral variability.

4. Discussion

The spectral variability hypothesis (SVH) provides a means of upscaling biodiversity assessments with remote sensing. Whereas the SVH has traditionally focused on terrestrial landscapes, it evidently can also be applied to seascapes. We demonstrated that fish diversity was positively correlated with spectral variation. Sensor type and the size of the window in which spectral variation was calculated, however, were important determinants in the strength of our correlations. These
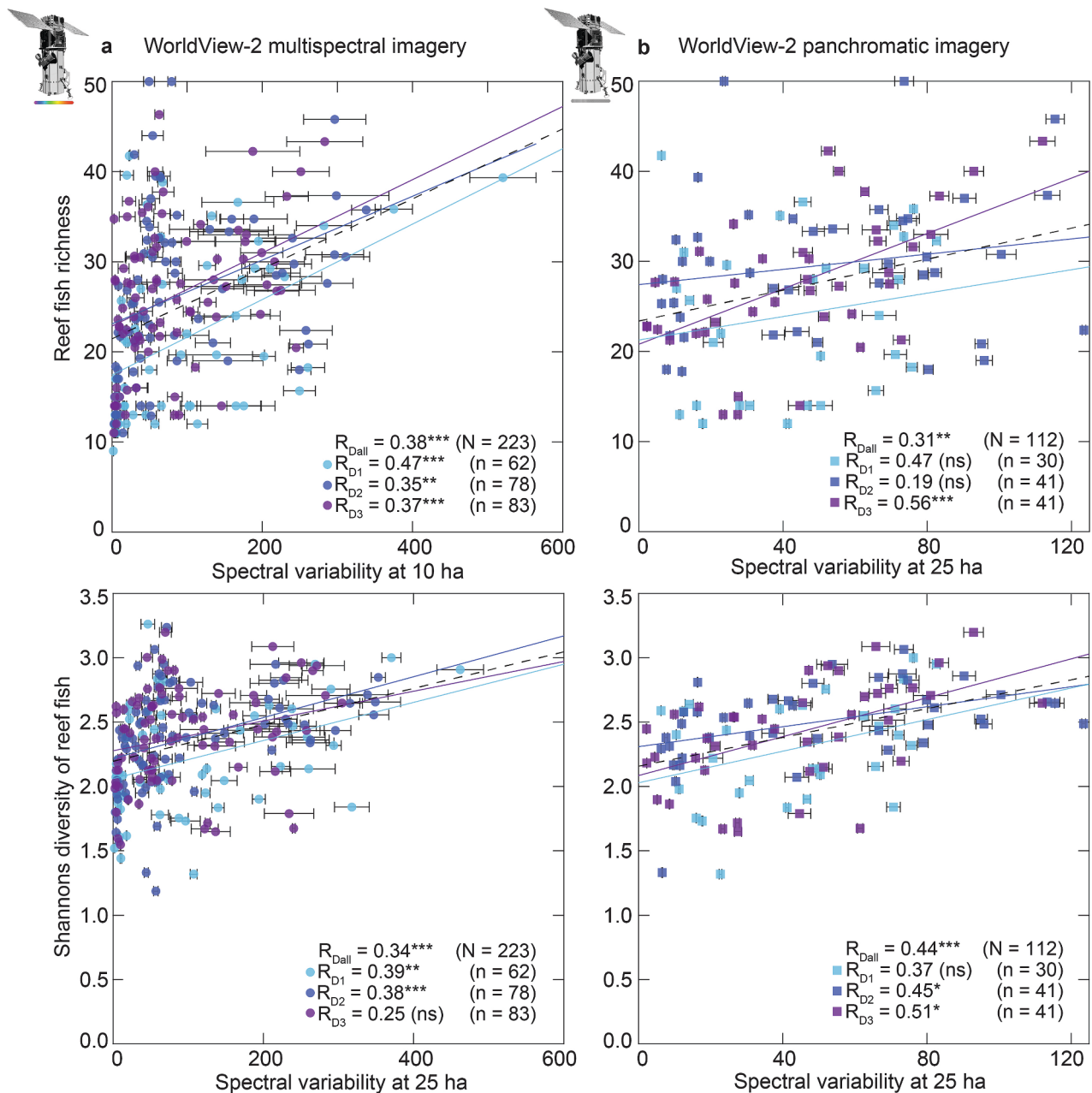
Fig. 4. Correlation plots showing the relationship between spectral variability to fish richness and Shannon's diversity for KSLOF-GRE stations. These results used the window sizes that delivered the strongest correlations for **(a)** WorldView-2 (WV-2) multispectral (10 and 25 ha, circles) and **(b)** panchromatic (10 ha, squares) imagery. Points colored by one of three depth classes (D1 is < 13 m, D2 is 13–15.5 m, and D3 > 15.5 m), with correlation strength (R) given for each. Error bars represented spectral variation around the center dive station, and for five random points within a 15-m radius. In all cases, correlation coefficients were significant and positive. The strongest relationship was between WV-2 panchromatic and Shannon's diversity of fish at D3 (>15.5 m).

nuances have also been discussed as being crucial when applying the SVH for terrestrial ecosystems (Torresani et al. 2018, 2024; Wang et al. 2018; Wang and Gamon 2019; Fassnacht et al. 2022), so we also unpack them below for coral reefs.

4.1. Pixel size matters

We pulled from three spatial scales of remote sensing imagery. At the coarse end, WV-2 had a 2.5 m resolution for its multispectral channels and 0.5 m for its panchromatic one. Fluid lensed images, with 0.014 m pixels, was finer in scale by a factor of 100. It was fair to say that the multispectral WV-2 data captured the arrangement of seabed 'habitat,' while panchromatic WV-2 data, and, to an even greater degree,

FluidCam, captured intra-habitat variability. The strongest correlations to fish diversity we found were delivered by panchromatic and Fluid-Cam imagery (Table 1, R = 0.44). This result insinuated that the SVH was upheld when spectral variation was captured at the intra-habitat scale. To understand this outcome, it was necessary to consider how an image of a coral reef was abstracted as its pixel size increased.

Sub-meter resolution images of reefs capture the spatial arrangement of individual coral colonies and the shadows that they cast. The 0.014 m-resolution of FluidCam even started to image the reef as it might have been experienced by a diver in the water, or a fish utilizing the habitat that it provided (Fig. 3d). In remote sensing terms, coral colonies (and their shadows) approximated to what ecologists often refer to as 'rugosity,' which a multitude of studies showed that reef fish respond to
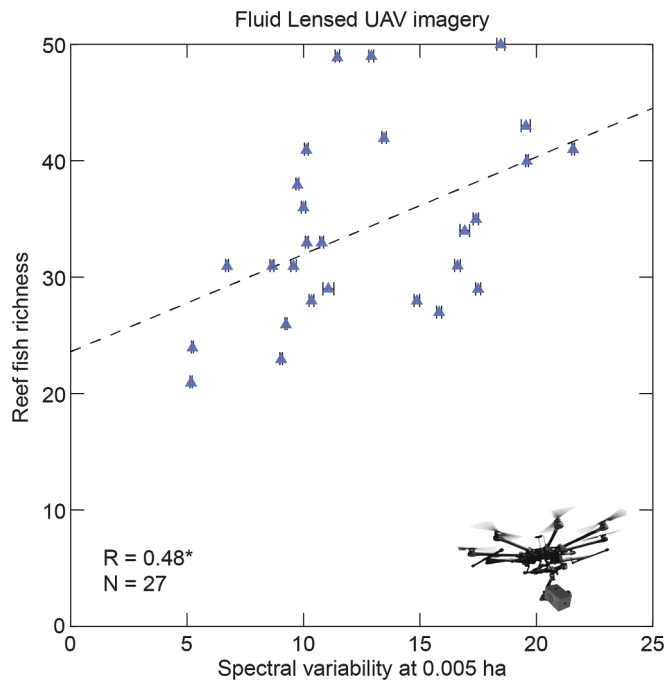
Fig. 5. Correlation plot showing the relationship between spectral variability from unpiloted aerial vehicle (UAV) fluid lensed imagery and fish richness across the GLTMP stations. Error bars represented the spectral variation around the center dive station, and for five random points within a 15-m radius. The strongest correlation was delivered by the largest 0.005 ha window size. No significant correlations were found between Shannon's diversity of fish and either the raw or the fluid lensed UAV data.

(Mazel et al. 2003; Gratwicke and Speight 2005; Purkis et al. 2006, 2008; Kobryn et al. 2013; Darling et al. 2017; Wedding et al. 2019; Foo et al. 2021; Hall and Kingsford 2021).

Though the scale jump from 0.014 m FluidCam and 0.5 m WV-2 panchromatic to 2.5 m WV-2 multispectral might not have seemed drastic, any semblance of rugosity was lost. Spectral variability at the WV-2 multispectral scale was mediated by the arrangement of benthic habitats – i.e., ecological communities, such as 'coral habitat,' 'seagrass,' 'sand habitat,' etc (Bakker et al. 2024). Although the seabed was no longer being measured at the scale of individual coral colonies, we still found fish diversity to be correlated with WV-2 multispectral variability, and at large window sizes, but our interpretation of the SVH at this scale was fundamentally different as compared to the cm-scale FluidCam imagery.

The literature advocated, however, that the relationship between fish and habitat was more nuanced than that between fish and rugosity. A handful of studies, for instance, showed that fish might have responded to habitat at WV-2 scale (Purkis et al. 2008; Yeager et al. 2011; Chong-Seng et al. 2012; Darling et al. 2017; Richardson et al. 2017; Bakker et al. 2024), but the direction and strength of those relationships varied. And, at these scales, habitat arrangement may have become homogenized within larger pixels, so that other environmental characteristics, instead, would be more important in structuring fish communities (Hewitt et al. 1998; Sale 1998; Holbrook et al. 2002). Cast in this way, it was hardly surprising that the strongest relationships which we found between spectral variability and fish (R = 0.44–0.48) were delivered at sub-meter scale.

4.2. The Spectral Variability Hypothesis weakens with increasing water depth

Basic physics decrees that light is exponentially attenuated with increasing water depth. Even more so, spectral diversity, while possibly present on the benthic surface at depth, is itself a function of depth owing to the differential attenuation of longer wavelengths of visible light in water. This attenuation sets a practical limit for passive remote sensing submerged targets in the visible spectrum of approximately 25 m (Purkis and Klemas 2011). So, a logical hypothesis for the strong correlations between fish and spectral variability were that they were depth dependent. Whereas the Guam FluidCam dataset was too small to offer meaningful statistical power, the KSLOF-GRE offered ample scope to test this simple hypothesis.

The KSLOF-GRE fish counts were conducted between water depths of 0–18 m, and our strongest correlations (R = 0.47 and 0.39) occurred in the shallowest depth bin (<13 m) when spectral variability was
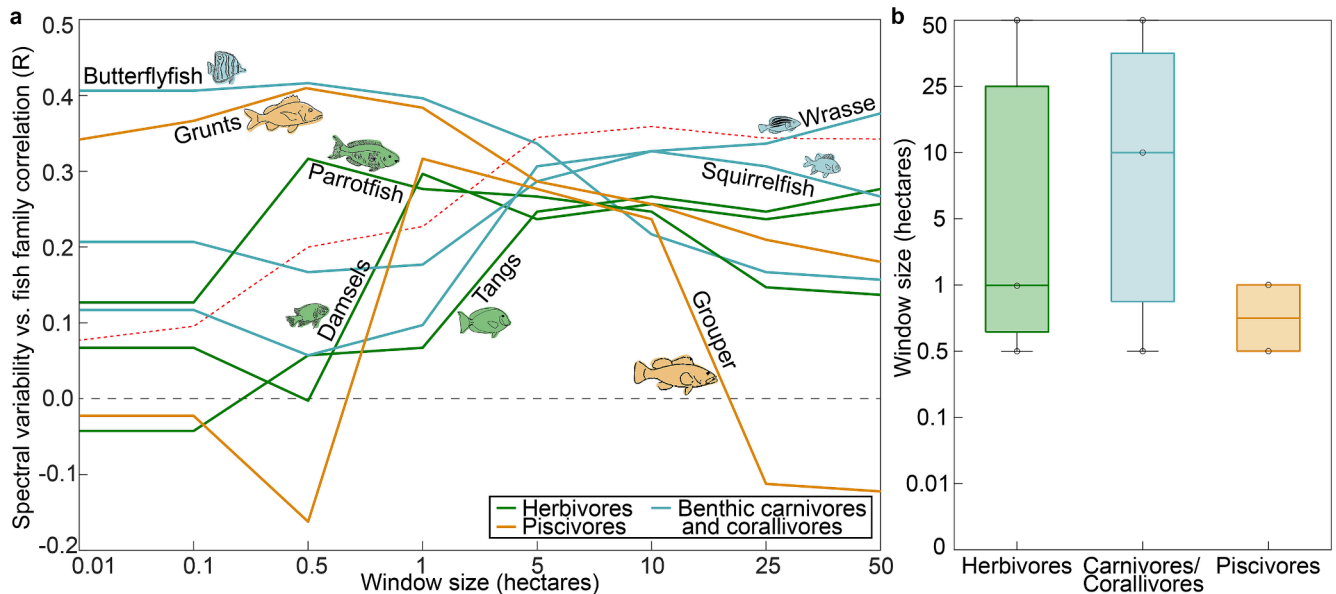

Fig. 6. The relationship between spectral variability with herbivores (green), benthic carnivores/corallivores (blue), and piscivores (orange) **(a)** was given for a range of windows sized from 0.01 to 50 ha. The red dashed line represented all fish families grouped together. The window size which delivered the peak correlations were shown in the box-and-whisker plot **(b)**. Piscivores were most strongly correlated to spectral variability across a narrow range of windows whereas the window sizes with peak correlations varied much more for herbivores and corallivores.

computed from multispectral WV-2 imagery. The deepest bin returned the weakest correlation for these multispectral data. For WV-2 panchromatic data, however, the deepest depth bin returned the strongest correlation (0.56 and 0.51). This result was confusing, and arbitrating the effect of depth on panchromatic data was challenging because the band spans visible and infrared wavelengths, thereby encompassing a broad disparity in the attenuation of light by water. While it has been shown that accuracy of classifying benthic habitats from imagery decreases with increasing water depth (Lucas and Goodman 2014; Garcia et al. 2018), a phenomenon termed 'spectral confusion,' no such information existed for the influence of depth on calculating Rao's Q values for the SVH. Although beyond the scope of this study, we encourage future research to investigate whether applying water-column corrections to remote sensing data enhances or undermines the effectiveness of the SVH as a proxy for reef fish biodiversity. Another suggestion is to trial the effect of pansharpening on correlation strength to further disentangle the relationship between fish and spectral information.

4.3. Fluid lensing outperformed raw UAV data

Unlike WV-2, the fluid lensing data offered the opportunity to correct for the light field projected onto the seabed by the lensing effect of ocean waves (caustics), magnification and demagnification of ocean wave lenslets, and reflective effects of ocean waves (Chirayath and Li 2019). This focused, reflected, and refracted sunlight did not originate from the seabed and therefore might be considered as noise in any computation of spectral diversity, particularly because water is dispersive, causing different wavelengths of refracted downwelling light to focus on different depths. Applying airborne fluid lensing, UAV data were explicitly corrected for all these effects (Fig. 3c vs. d). Our strongest correlations between spectral variability and fish were realized when using the fluid lensed data, and no relationships were found with the raw imagery. This finding has important implications for the use of spectral variability from any remote sensing system that does not correct for refractive distortions, caustics, or dispersion. However, we acknowledge that the dataset we used to produce these results was small. Our findings cannot necessarily be extrapolated to other reefs. This said, at our sites, acquisition of UAV data with fluid lensing clearly paid dividends in the retrieval of fish biodiversity.

4.4. The Spectral Variability Hypothesis worked for some fish better than others

We attempted to tease apart the relationship between fish and their surrounding spectral diversity by splitting fish into herbivores, corallivores, and piscivores. Peak correlations for herbivorous fish spanned window sizes from 0.5 to 50 ha, perhaps reflecting the variety of ranges that encompassed the life stages of herbivorous fish. For example, some surgeonfish (tangs) and parrotfish aggressively defend their breeding or feeding territories that are only 1–20 m across, while some unicornfish (also tangs) range up to 1 km (Green et al. 2015). The butterflyfish exhibited the strongest correlations at <0.5 ha windows, which could have been due to the fact that some species (e.g., clownfish and butterflyfish) exhibit self-recruitment behavior where their larvae disperse over distances as little as 10 m (Almany et al., 2007). We also found piscivores to have stronger correlations within smaller windows, potentially because these are ambush predators. Their feeding behavior is to sit and wait in one area. The variability we saw between the window sizes which delivered the peak correlations for specific fish families highlighted the value of incorporating habitat diversity and connectivity into conservation planning, because, even though we included site-attached damsels and butterflyfish, the box-and-whisker plots in Fig. 6b suggested that the fish were responding to spectral signatures over half a kilometer away (50 ha windows).

5. Conclusion

We demonstrated the applicability of the spectral variability hypothesis in marine environments using WorldView-2 multispectral and panchromatic and UAV imagery. The positive correlations between spectral variability and fish diversity showed the potential for remote sensing to upscale biodiversity assessments, especially with imagery processed with fluid lensing corrections. The resolution of the imagery also impacted the strength of those correlations, with smaller pixels generally yielding stronger relationships. We also found the effectiveness of the SVH to vary with water depth and for different fish feeding strategies, indicating the need for a tailored approach to apply this hypothesis depending on the management goal. Our findings support a broader utilization of remote sensing in marine biodiversity conservation.

efforts of the Guam Long-term Coral Reef Monitoring Program team, who provided us with field data through the NOAA Coral Reef Conservation Program. Our appreciation extends to Sara Al-Balushi for her expert refinement and enhancement of our figures. Lastly, we are grateful for the insightful feedback from two anonymous reviewers and Editor-in-Chief Giovanni Zurlini.

Data availability

Data will be made available on request.

References

Almany, G.R., Berumen, M.L., Thorrold, S.R., Planes, S., Jones, G.P., 2007. Local replenishment of coral reef fish populations in a marine reserve. Science 316, 742–744.

Alvarez-Filip, L., Dulvy, N.K., Gill, J.A., Côté, I.M., Watkinson, A.R., 2009. Flattening of Caribbean coral reefs: Region-wide declines in architectural complexity. Proc. R. Soc. B Biol. Sci. 276, 3019–3025.

Ault, J.S., Smith, S.G., Bohnsack, J.A., Luo, J., Harper, D.E., McClellan, D.B., 2006. Building sustainable fisheries in Florida's coral reef ecosystem: Positive signs in the Dry Tortugas. Bull. Mar. Sci. 78, 633–654.

Bachman, S., Green, R., Bakker, A., Fox, H., Purkis, S., Harshbarger, B., 2023. High-performance programming and execution of a coral biodiversity mapping algorithm using Chapel. Proceedings of the SC '23 Workshops of the International Conference on High Performance Computing and Analysis 1162–1170.

Bakker, A.C., Gleason, A.C.R., Mantero, A., Dempsey, A.C., Andréfouët, S., Harborne, A. R., Purkis, S.J., 2022. Heat, human, hydrodynamic, and habitat drivers measured from space correlate with metrics of reef health across the South Pacific. Coral Reefs 1, 1–20.

Bakker, A.C., Gleason, A.C.R., Dempsey, A.C., Fox, H.E., Green, R.H., Purkis, S.J., 2024. Remotely sensed habitat diversity predicts species diversity on coral reefs. Remote Sens. Environ. 302, 113990.

Beveridge, M.C.M., Thilsted, S.H., Phillips, M.J., Metian, M., Troell, M., Hall, S.J., 2013. Meeting the food and nutrition needs of the poor: The role of fish and the opportunities and challenges emerging from the rise of aquaculture. J. Fish Biol. 83, 1067–1084.

Brown, J.H., 1984. On the relationship between abundance and distribution of species. Am. Nat. 124, 255–279.

Burdick, D., Raymundo, L., Drake, D., Hershberger, A., 2023. A decade of change on Guam's coral reefs. University of Guam Marine Laboratory, In Guam Coral Reef Initiative Resources.

Carlson, K.M., Asner, G.P., Hughes, R.F., Ostertag, R., Martin, R.E., 2007. Hyperspectral remote sensing of canopy biodiversity in Hawaiian lowland rainforests. Ecosystems 10, 536–549.

Chirayath, V., Earle, S.A., 2016. Drones that see through waves - preliminary results from airborne fluid lensing for centimetre-scale aquatic conservation. Aquat. Conserv. 26, 237–250.

Chirayath, V., Instrella, R., 2019. Fluid lensing and machine learning for centimeter-resolution airborne assessment of coral reefs in American Samoa. Remote Sens. Environ. 235, 111475.

Chirayath, V., Li, A., 2019. Next-generation optical sensing technologies for exploring ocean worlds—NASA FluidCam, MiDAR, and NeMO-Net. Front. Mar. Sci. 6, 521.

Chong-Seng, K.M., Mannering, T.D., Pratchett, M.S., Bellwood, D.R., Graham, N.A.J., 2012. The influence of coral reef benthic condition on associated fish assemblages. PLoS One 7, e42167.

Collin, A., Planes, S., 2012. Enhancing coral health detection using spectral diversity indices from WorldView-2 imagery and machine learners. Remote Sens. (Basel) 4, 3244–3264.

Cox, C., Woods, M.B., Reimchen, T.E., 2021. Regional heterogeneity in coral species richness and hue reveals novel global predictors of reef fish intra-family diversity. Sci. Rep. 11, 1–12.

Dalleau, M., Andréfouët, S., Wabnitz, C.C., Payri, C., Wantiez, L., Pichon, M., Friedman, K., Vigliola, L., Benzoni, F., 2010. Use of habitats as surrogates of biodiversity for efficient coral reef conservation planning in Pacific Ocean islands. Conserv. Biol. 24, 541–552.

Darling, E.S., Graham, N.A.J., Januchowski-Hartley, F.A., Nash, K.L., Pratchett, M.S., Wilson, S.K., 2017. Relationships between structural complexity, coral traits, and reef fish assemblages. Coral Reefs 36, 561–575.

Díaz-Pérez, L., Rodríguez-Zaragoza, F.A., Ortiz, M., Cupul-Magaña, A.L., Carriquiry, J.D., Ríos-Jara, E., Rodríguez-Troncoso, A.P., Del Carmen, G.-R., 2016. Coral reef health indices versus the biological, ecological and functional diversity of fish and coral assemblages in the Caribbean Sea. PLoS One 11, e0161812.

DigitalGlobe, DigitalGlobe Core Imagery Products Guide https://www.geosoluciones.cl/documentos/worldview/DigitalGlobe-Core-Imagery-Products-Guide.pdf 2021 Accessed 2023.

English, S.A., Wilkinson, C., Baker, V.J., 1997. Survey manual for tropical marine resources. Australian Institute of Marine Science, Townsville.

Fassnacht, F.E., Müllerová, J., Conti, L., Malavasi, M., Schmidtlein, S., 2022. About the link between biodiversity and spectral variation. Appl. Veg. Sci. 25, e12643.

Foo, S.A., Walsh, W.J., Lecky, J., Marcoux, S., Asner, G.P., 2021. Impacts of pollution, fishing pressure, and reef rugosity on resource fish biomass in West Hawaii. Ecol. Appl. 31, e2213.

Fukunaga, A., Kosaki, R.K., Pascoe, K.H., Burns, J.H.R., 2020. Fish assemblage structure in the Northwestern Hawaiian Islands is associated with the architectural complexity of coral-reef habitats. Diversity (Basel) 12, 430.

Garcia, R.A., Lee, Z., Hochberg, E.J., 2018. Hyperspectral shallow-water remote sensing with an enhanced benthic classifier. Remote Sens. (Basel) 10, 147.

Gholizadeh, H., Dixon, A.P., Pan, K.H., McMillan, N.A., Hamilton, R.G., Fuhlendorf, S.D., Cavender-Bares, J., Gamon, J.A., 2022. Using airborne and DESIS imaging spectroscopy to map plant diversity across the largest contiguous tract of tallgrass prairie on earth. Remote Sens. Environ. 281, 113254.

Global Reef Expedition Final Report, 2021. Carlton, R., Dempsey, A., Thompson, L., Heemsoth, A., Lubarsky, K., Faisal, M., Purkis, S. Khaled bin Sultan Living Oceans Foundation, Annapolis, MD. vol. 15.

Goetz, S., Steinberg, D., Dubayah, R., Blair, B., 2007. Laser remote sensing of canopy habitat heterogeneity as a predictor of bird species richness in an eastern temperate forest, USA. Remote Sens. Environ. 108, 254–263.

Graham, N.A.J., Nash, K.L., 2013. The importance of structural complexity in coral reef ecosystems. Coral Reefs 32, 315–326.

Gratwicke, B., Speight, M.R., 2005. The relationship between fish species richness, abundance and habitat complexity in a range of shallow tropical marine habitats. J. Fish Biol. 66, 650–667.

Green, A.L., Maypa, A.P., Almany, G.R., Rhodes, K.L., Weeks, R., Abesamis, R.A., Gleason, M.G., Mumby, P.J., White, A.T., 2015. Larval dispersal and movement patterns of coral reef fishes, and implications for marine reserve network design. Biol. Rev. 90, 1215–1247.

Green, E., Mumby, P., Edwards, A., Clark, C., 2000. Remote sensing: Handbook for tropical coastal management. United Nations Educational, Scientific and Cultural Organization (UNESCO).

Hale, R., Colton, M.A., Peng, P., Swearer, S.E., 2019. Do spatial scale and life history affect fish–habitat relationships? J. Anim. Ecol. 88, 439–449.

Hall, K., Johansson, L.J., Sykes, M.T., Reitalu, T., Larsson, K., Prentice, H.C., 2010. Inventorying management status and plant species richness in semi-natural grasslands using high spatial resolution imagery. Appl. Veg. Sci. 13, 221–233.

Hall, A.E., Kingsford, M.J., 2021. Habitat type and complexity drive fish assemblages in a tropical seascape. J. Fish Biol. 99, 1364–1379.

Hall, K., Reitalu, T., Sykes, M.T., Prentice, H.C., 2012. Spectral heterogeneity of QuickBird satellite data is related to fine-scale plant species spatial turnover in semi-natural grasslands. Appl. Veg. Sci. 15, 145–157.

Hauser, L.T., Timmermans, J., van der Windt, N., Sil, Â.F., César de Sá, N., Soudzilovskaia, N.A., van Bodegom, P.M., 2021. Explaining discrepancies between spectral and *in-situ* plant diversity in multispectral satellite earth observation. Remote Sens. Environ. 265, 112684.

Hedley, J.D., Mumby, P.J., Joyce, K.E., Phinn, S.R., 2004. Spectral unmixing of coral reef benthos under ideal conditions. Coral Reefs 23, 60–73.

Heenan, A., Williams, I.D., Acoba, T., DesRochers, A., Kosaki, R.K., Kanemura, T., Nadon, M.O., Brainard, R.E., 2017. Long-term monitoring of coral reef fish assemblages in the Western Central Pacific. Sci. Data 4, 1–12.

Heumann, B.W., Hackett, R.A., Monfils, A.K., 2015. Testing the spectral diversity hypothesis using spectroscopy data in a simulated wetland community. Ecol Inform 25, 29–34.

Hewitt, J.E., Thrush, S.F., Cummings, V.J., Turner, S.J., 1998. The effect of changing sampling scales on our ability to detect effects of large-scale processes on communities. J. Exp. Mar. Biol. Ecol. 227, 251–264.

Holbrook, S.J., Brooks, A.J., Schmitt, R.J., 2002. Predictability of fish assemblages on coral patch reefs. Mar. Freshw. Res. 53, 181–188.

Jankowski, M.W., Gardiner, N.R., Jones, G.P., 2015. Depth and reef profile: Effects on the distribution and abundance of coral reef fishes. Environ. Biol. Fishes 98, 1373–1386.

Kawarazuka, N., Béné, C., 2011. The potential role of small fish species in improving micronutrient deficiencies in developing countries: Building evidence. Public Health Nutr. 14, 1927–1938.

Kerr, J.M., Purkis, S., 2018. An algorithm for optically-deriving water depth from multispectral imagery in coral reef landscapes in the absence of ground-truth data. Remote Sens. Environ. 210, 307–324.

Khare, S., Latifi, H., Rossi, S., 2019. Forest beta-diversity analysis by remote sensing: How scale and sensors affect the Rao's Q index. Ecol. Ind. 106, 105520.

Kobryn, H.T., Wouters, K., Beckley, L.E., Heege, T., 2013. Ningaloo Reef: Shallow marine habitats mapped using a hyperspectral sensor. PLoS One 8, e70105.

Kutser, T., Hedley, J., Giardino, C., Roelfsema, C., Brando, V.E., 2020. Remote sensing of shallow waters – A 50 year retrospective and future directions. Remote Sens. Environ. 240, 111619.

Lee, Z., Carder, K.L., Mobley, C.D., Steward, R.G., Patch, J.S., 1999. Hyperspectral remote sensing for shallow waters: 2. Deriving bottom depths and water properties by optimization. Appl. Opt. 38, 3831–3843.

Lengyel, S., Déri, E., Magura, T., 2016. Species richness responses to structural or compositional habitat diversity between and within grassland patches: A multi-taxon approach. PLoS One 11, e0149662.

Li, J., Fabina, N.S., Knapp, D.E., Asner, G.P., 2020. The sensitivity of multi-spectral satellite sensors to benthic habitat change. Remote Sens. (Basel) 12, 532.

Lucas, M.Q., Goodman, J., 2014. Linking coral reef remote sensing and field ecology: It's a matter of scale. J Mar Sci Eng 3, 1–20.

Lyzenga, D.R., 1978. Passive remote sensing techniques for mapping water depth and bottom features. Appl. Opt. 17, 379–383.

MacArthur, R.H., MacArthur, J.W., 1961. On bird species diversity. Ecology 42, 594–598.

Mazel, C.H., Strand, M.P., Lesser, M.P., Crosby, M.P., Coles, B., Nevis, A.J., 2003. High-resolution determination of coral reef bottom cover from multispectral fluorescence laser line scan imagery. Limnol. Oceanogr. 48, 522–534.

McElhinny, C., Gibbons, P., Brack, C., Bauhus, J., 2005. Forest and woodland stand structural complexity: Its definition and measurement. For. Ecol. Manage. 218, 1–24.

McPartland, M.Y., Falkowski, M.J., Reinhardt, J.R., Kane, E.S., Kolka, R., Turetsky, M.R., Douglas, T.A., Anderson, J., Edwards, J.D., Palik, B., Montgomery, R.A., 2019. Characterizing boreal peatland plant composition and species diversity with hyperspectral remote sensing. Remote Sens. 11, 1685.

Oldeland, J., Wesuls, D., Rocchini, D., Schmidt, M., Jürgens, N., 2010. Does using species abundance data improve estimates of species diversity from remotely sensed spectral heterogeneity? Ecol. Ind. 10, 390–396.

Olds, A.D., Connolly, R.M., Pitt, K.A., Maxwell, P.S., 2012. Primacy of seascape connectivity effects in structuring coral reef fish assemblages. Mar. Ecol. Prog. Ser. 462, 191–203.

Pacheco-Labrador, J., Migliavacca, M., Ma, X., Mahecha, M., Carvalhais, N., Weber, U., Benavides, R., Bouriaud, O., Barnoaiea, I., Coomes, D.A., Bohn, F.J., Kraemer, G., Heiden, U., Huth, A., Wirth, C., 2022. Challenging the link between functional and spectral diversity with radiative transfer modeling and data. Remote Sens. Environ. 280, 113170.

Palmer, M.W., Earls, P.G., Hoagland, B.W., White, P.S., Wohlgemuth, T., 2002. Quantitative tools for perfecting species lists. Environmetrics 13, 121–137.

Palmer, M.W., Wohlgemuth, T., Earls, P., Arévalo, J.R., Thompson, S.D., 1999. Opportunities for long-term ecological research at the Tallgrass Prairie Preserve, Oklahoma. Budapest, Hungary.

Pratchett, M.S., Thompson, C.A., Hoey, A.S., Cowman, P.F., Wilson, S.K., 2018. Effects of coral bleaching and coral loss on the structure and function of reef fish assemblages. Springer, Cham, pp. 265–293.

Purkis, S., Chirayath, V., 2022. Remote sensing the ocean biosphere. Annu. Rev. Env. Resour. 47, 823–847.

Purkis, S.J., Graham, N.A.J., Riegl, B.M., 2008. Predictability of reef fish diversity and abundance using remote sensing data in Diego Garcia (Chagos Archipelago). Coral Reefs 27, 167–178.

Purkis, S.J., Gleason, A.C.R., Purkis, C.R., Dempsey, A.C., Renaud, P.G., Faisal, M., Saul, S., Kerr, J.M., 2019. High-resolution habitat and bathymetry maps for 65,000 sq. km of Earth's remotest coral reefs. Coral Reefs 38, 467–488.

Purkis, S.J., Klemas, V.V., 2011. Remote sensing and global environmental change. John Wiley & Sons.

Purkis, S.J., Kohler, K.E., 2008. The role of topography in promoting fractal patchiness in a carbonate shelf landscape. Coral Reefs 27, 977–989.

Purkis, S.J., Myint, S.W., Riegl, B.M., 2006. Enhanced detection of the coral *Acropora cervicornis* from satellite imagery using a textural operator. Remote Sens. Environ. 101, 82–94.

Putkiranta, P., Räsänen, A., Korpelainen, P., Erlandsson, R., Kolari, T.H.M., Pang, Y., Villoslada, M., Wolff, F., Kumpula, T., Virtanen, T., 2024. The value of hyperspectral UAV imagery in characterizing tundra vegetation. Remote Sens. Environ. 308, 114175.

Richardson, L.E., Graham, N.A.J., Pratchett, M.S., Hoey, A.S., 2017. Structural complexity mediates functional structure of reef fish assemblages among coral habitats. Environ. Biol. Fishes 100, 193–207.

Richardson, L.E., Graham, N.A.J., Pratchett, M.S., Eurich, J.G., Hoey, A.S., 2018. Mass coral bleaching causes biotic homogenization of reef fish assemblages. Glob. Chang. Biol. 24, 3117–3129.

Riegl, B.M., Purkis, S.J., Al-Cibahy, A.S., Al-Harthi, S., Grandcourt, E., Al-Sulaiti, K., Baldwin, J., Abdel-Moati, A.M., 2012. Coral bleaching and mortality thresholds in the SE Gulf: Highest in the world. Adaptation to climatic extremes, Coral reefs of the Gulf, pp. 95–105.

Rocchini, D., Chiarucci, A., Loiselle, S.A., 2004. Testing the spectral variation hypothesis by using satellite multispectral images. Acta Oecol. 26, 117–120.

Rocchini, D., Ricotta, C., Chiarucci, A., 2007. Using satellite imagery to assess plant species richness: The role of multispectral systems. Appl. Veg. Sci. 10, 325–331.

Rocchini, D., Dadalt, L., Delucchi, L., Neteler, M., Palmer, M.W., 2014. Disentangling the role of remotely sensed spectral heterogeneity as a proxy for North American plant species richness. Community Ecol. 15, 37–43.

Rocchini, D., Marcantonio, M., Ricotta, C., 2017. Measuring Rao's Q diversity index from remote sensing: An open source solution. Ecol. Ind. 72, 234–238.

Rogers, A., Blanchard, J.L., Mumby, P.J., 2014. Vulnerability of coral reef fisheries to a loss of structural complexity. Curr. Biol. 24, 1000–1005.

Rogers, A., Harborne, A.R., Brown, C.J., Bozec, Y.M., Castro, C., Chollett, I., Hock, K., Knowland, C.A., Marshell, A., Ortiz, J.C., Razak, T., Roff, G., Samper-Villarreal, J., Saunders, M.I., Wolff, N.H., Mumby, P.J., 2015. Anticipative management for coral reef ecosystem services in the 21st century. Glob. Chang. Biol. 21, 504–514.

Rossi, C., Kneubühler, M., Schütz, M., Schaepman, M.E., Haller, R.M., Risch, A.C., 2022. Spatial resolution, spectral metrics and biomass are key aspects in estimating plant species richness from spectral diversity in species-rich grasslands. Remote Sens. Ecol. Conserv. 8, 297–314.

Rowlands, G.P., Purkis, S.J., Riegl, B.M., 2008. The 2005 coral-bleaching event Roatan (Honduras): Use of pseudoinvariant features (PIFs) in satellite assessments. J. Spat. Sci. 53, 99–112.

Sale, P.F., 1998. Appropriate spatial scales for studies of reef-fish ecology. Aust. J. Ecol. 23, 202–208.

Schmidtlein, S., Fassnacht, F.E., 2017. The spectral variability hypothesis does not hold across landscapes. Remote Sens. Environ. 192, 114–125.

Shannon, C.E., 1948. A mathematical theory of communication. Bell Syst. Tech. J. 27, 379–423.

Sievers, K.T., McClure, E.C., Abesamis, R.A., Russ, G.R., 2020. Non-reef habitats in a tropical seascape affect density and biomass of fishes on coral reefs. Ecol. Evol. 10, 13673.

Stein, A., Gerstner, K., Kreft, H., 2014. Environmental heterogeneity as a universal driver of species richness across taxa, biomes and spatial scales. Ecol. Lett. 17, 866–880.

Stumpf, R.P., Holderied, K., Sinclair, M., 2003. Determination of water depth with high-resolution satellite imagery over variable bottom types. Limnol. Oceanogr. 48, 547–556.

Syms, C., Jones, G.P., 1998. Disturbance, habitat structure and the ecology of fishes on coral reefs. Austral Ecol. 23, 287–297.

Torresani M, Rocchini D, Zebisch M, Sonnenschein R, Tonon G (2018) Testing the spectral variation hypothesis by using the Rao-Q index to estimate forest biodiversity: Effect of spatial resolution. International Geoscience and Remote Sensing Symposium (IGARSS) 2018-July:1183–1186.

Torresani, M., Rocchini, D., Sonnenschein, R., Zebisch, M., Marcantonio, M., Ricotta, C., Tonon, G., 2019. Estimating tree species diversity from space in an alpine conifer forest: The Rao's Q diversity index meets the spectral variation hypothesis. Ecol Inform 52, 26–34.

Torresani, M., Rossi, C., Perrone, M., Hauser, L.T., Féret, J.B., Moudrý, V., Simova, P., Ricotta, C., Foody, G.M., Kacic, P., Feilhauer, H., Malavasi, M., Tognetti, R., Rocchini, D., 2024. Reviewing the Spectral Variation Hypothesis: Twenty years in the tumultuous sea of biodiversity estimation by remote sensing. Ecol. Inform. 82, 102702.

University of Guam Marine Laboratory, 2019. Guam Long-term Coral Reef Monitoring Program Coral Colony Size and Condition Surveys Since 2010. NOAA's National Center for Environmental Information, https://www.fisheries.noaa.gov/inport/item/47781.

van Lier, J.R., Wilson, S.K., Depczynski, M., Wenger, L.N., Fulton, C.J., 2018. Habitat connectivity and complexity underpin fish community structure across a seascape of tropical macroalgae meadows. Landsc. Ecol. 33, 1287–1300.

Wang, R., Gamon, J.A., 2019. Remote sensing of terrestrial plant biodiversity. Remote Sens. Environ. 231, 111218.

Wang, R., Gamon, J.A., Cavender-Bares, J., Townsend, P.A., Zygielbaum, A.I., 2018. The spatial sensitivity of the spectral diversity-biodiversity relationship: An experimental test in a prairie grassland. Ecol. Appl. 28, 541–556.

Wedding, L.M., Jorgensen, S., Lepczyk, C.A., Friedlander, A.M., 2019. Remote sensing of three-dimensional coral reef structure enhances predictive modeling of fish assemblages. Remote Sens. Ecol. Conserv. 2, 150–159.

Williams, I.D., Richards, B.L., Sandin, S.A., Baum, J.K., Schroeder, R.E., Nadon, M.O., Zgliczynski, B., Craig, P., McIlwain, J.L., Brainard, R.E., 2011. Differences in reef fish assemblages between populated and remote reefs spanning multiple archipelagos across the central and western Pacific. Journal of Marine Sciences 2011, 826234.

Wilson, S.K., Fisher, R., Pratchett, M.S., Graham, N.A.J., Dulvy, N.K., Turner, R.A., Cakacaka, A., Polunin, N.V.C., 2010. Habitat degradation and fishing effects on the size structure of coral reef fish communities. Ecol. Appl. 20, 442–451.

Yanovski, R., Nelson, P.A., Abelson, A., 2017. Structural complexity in coral reefs: Examination of a novel evaluation tool on different spatial scales. Front. Ecol. Evol. 5, 27.

Yeager, L.A., Layman, C.A., Allgeier, J.E., 2011. Effects of habitat heterogeneity at multiple spatial scales on fish community assembly. Oecologia 167, 157–168.